

# Chemical mechanism of surface-enhanced resonance Raman scattering via charge transfer in pyridine–Ag<sub>2</sub> complex

Mengtao Sun,<sup>1\*</sup> Songbo Wan,<sup>1,2</sup> Yajun Liu,<sup>3</sup> Yu Jia<sup>2</sup> and Hongxing Xu<sup>1,4</sup>

<sup>1</sup> Beijing National Laboratory for Condensed Matter Physics, State Key Laboratory for Surface Physics, Institute of Physics, Chinese Academy of Sciences, Beijing, 100080, P. R. China

<sup>2</sup> Physical Science and Technology College, Zhengzhou University, Zhengzhou, P. R. China

<sup>3</sup> College of Chemistry, Beijing Normal University, Beijing, 100875, P. R. China

<sup>4</sup> Division of Solid State Physics, Lund University, Lund 22100, Sweden

Received 24 June 2007; Accepted 16 August 2007

A theoretical model is presented to describe the chemical mechanism of surface-enhanced resonance Raman scattering (SERRS) via charge transfer (CT) in the pyridine–Ag<sub>2</sub> complex. We first describe the influence of the interaction between the metal cluster and pyridine to the ground-state properties of the pyridine–Ag<sub>2</sub> complex, such as charge redistribution, the change of the atomic-resolved density of state, and the change of energy levels of occupied and unoccupied molecular orbitals. Second, we visualize the CT between the metal cluster and pyridine and within the intracuster on the electronic state transitions with charge difference density. The CT between the metal cluster and pyridine is the direct evidence of chemical mechanism for SERRS. Third, the spectra of SERRS are calculated with different incident light wavelengths that resonate with the different electronic state energy levels, and the enhanced intensities of different vibrational modes are compared, which show that there are different enhancement rates for different vibrational modes. Strong Raman scattering can be achieved not only by the CT between pyridine and the metal cluster but also by electronic intracuster excitation via a type of Förster excitation transfer, and the latter results from the local field effects by collective plasmons. The selection rules for the SERRS have been obtained for these two types of enhanced mechanisms. Copyright © 2008 John Wiley & Sons, Ltd.

**KEYWORDS:** chemical mechanism via charge transfer; SERRS; charge difference density; collective plasmons; Förster excitation transfer

## INTRODUCTION

Thirty years after the discovery of surface-enhanced Raman scattering (SERS),<sup>1,2</sup> it is generally accepted that the enormous enhancement of the Raman signal is due mainly to two types of mechanisms. The first is the electromagnetic (EM) enhancement, which is caused by the strong surface plasmon resonance of the rough metal surface coupled to the incident light.<sup>2–5</sup> The second is the chemical enhancement,<sup>6–26</sup> which can be considered similar to a resonance Raman process between the ground electronic state of the molecule–metal complex and its new excited levels arising from charge transfer (CT) between the metallic

surface and the adsorbed molecule. Apart from a factor of 10–10<sup>4</sup> chemical enhancement,<sup>16,17</sup> the Raman wavenumbers of molecule–metal complex are also usually different from those of the molecule.

In this paper, we present the chemical mechanisms of surface-enhanced resonance Raman scattering (SERRS) based on the experimental and theoretical reports.<sup>16–27</sup> Through visualization we theoretically investigate how CT occurs in the molecule–metal complex with our developed code of charge difference density,<sup>28–30</sup> which shows visually the orientation and result of the CT between pyridine and the Ag cluster in photoinduced dynamics. With difference in charge density, electronic intracuster excitations with strong oscillator strengths are also shown. The strong Raman scattering can be achieved not only by the CT between pyridine and the metal cluster but also by electronic intracuster excitation via a type of Förster excitation transfer.

\*Correspondence to: Mengtao Sun, Beijing National Laboratory for Condensed Matter Physics, State Key Laboratory for Surface Physics, Institute of Physics, Chinese Academy of Sciences, Beijing, 100080, P. R. China. E-mail: mtsun@aphy.iphy.ac.cn

The selection rules for the SERRS have been obtained for these two types of enhanced mechanisms.

### THEORETICAL METHOD

All the quantum chemical calculations were performed with the Gaussian 03 suite.<sup>31</sup> The ground state geometry of pyridine was optimized by means of the density functional theory (DFT), Becke's three-parameter hybrid functional with the nonlocal correlation of Lee–Yang–Parr (B3LYP) along with the 6-31G(D) basis set. The optical spectrum of pyridine was derived by the TD-DFT, B3LYP/6-31G(D) method. For quantum chemical calculations, the complex of pyridine and small Ag clusters is used. We assume that the pyridine molecule interacts with Ag clusters along the bond axis so that the pyridine–Ag complex keeps the C<sub>2v</sub> symmetry point group (Fig. 1). In the process of normal mode analysis, the C<sub>2v</sub> symmetric configuration has the advantage that the group representations of the vibrational modes remain invariable in the pyridine–Ag complex.<sup>32</sup> The geometry optimization and wavenumber analysis of pyridine–Ag<sub>2</sub> for the ground states were performed with DFT, B3LYP functional, and the LanL2DZ basis set. Optical spectra of pyridine–Ag were calculated by the TD-DFT method with the same functional and basis set. Absolute off- and on-resonance Raman intensities can be calculated as the differential Raman scattering cross-section. For Stokes scattering with an experimental setup of a 90° scattering angle

and perpendicular plane-polarized light, the cross-section is written as:<sup>33</sup>

$$\frac{d\sigma}{d\Omega} = \frac{\pi^2}{\varepsilon_0^2} (\omega_{\text{in}} - \omega_p)^4 \frac{h}{8\pi^2 c \omega_p} S_p \frac{1}{45[1 - \exp(-hc\omega_p/k_B T)]} \quad (1)$$

where  $\omega_{\text{in}}$  and  $\omega_p$  are the frequency of the incident light and of the  $p$ th vibrational mode, respectively, and  $S_p$  is the Raman scattering factor (or Raman activity in unit A<sup>4</sup>/amu; note that amu is not the mass unit in atomic units but the so-called (unified) atomic mass unit, which is sometimes denoted as  $u = (1/12)m(^{12}\text{C}) = 10^{-3}\text{kg mol}^{-1} N_A$ ).<sup>33</sup>

$$S_p = 45 \left( \frac{\partial \alpha}{\partial Q_p} \right)^2 + 7 \left( \frac{\partial \gamma}{\partial Q_p} \right)^2 \quad (2)$$

which is a pure molecular property and independent of experimental setup.  $\alpha_p$  and  $\gamma_p$  are the isotropic and anisotropic polarizabilities. In this paper,  $S_p$  values were directly calculated by Gaussian 03 suite.<sup>31</sup>

### RESULTS AND DISCUSSION

Comparing the atomic-resolved density of state (DOS) of pyridine with that of pyridine–Ag<sub>2</sub> (Fig. 2), the orbital energy levels of occupied molecular orbitals of pyridine–Ag<sub>2</sub> increase, while that of the unoccupied molecular orbitals decrease, and therefore the corresponding band gap (energy difference between HOMO and LUMO, where HOMO and LUMO stand for the highest occupied and lowest unoccupied molecular orbitals, respectively) of pyridine–Ag<sub>2</sub> decreases, which can be interpreted by the renormalization of molecular electronic levels at the metal–molecule interface.<sup>34</sup> The DOS in Fig. 2(b) shows that the densities of HOMO – 1, HOMO, and LUMO + 2 are almost totally distributed on Ag, while the densities of LUMO and LUMO + 1 are almost totally distributed on the pyridine. The interaction between Ag and pyridine also results in (1) Mulliken charge redistribution and electron transfer from pyridine to Ag,  $\Delta e = 0.158$  (there are 0.158 net electrons on Ag<sub>2</sub> cluster) and (2) the increase of the static dipole moment and polarizability of

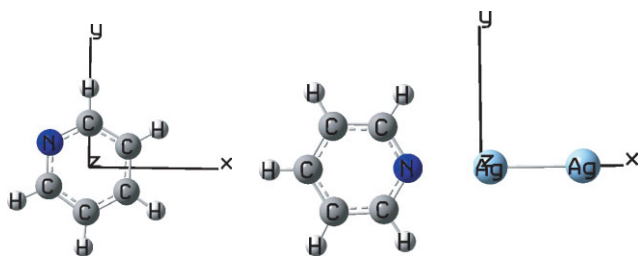


**Figure 1.** Chemical structures of pyridine and pyridine–Ag<sub>2</sub> with their Cartesian coordinates.

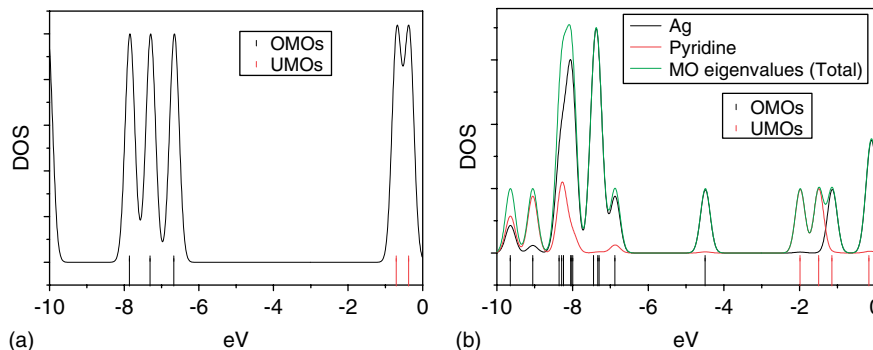


**Figure 2.** The atomic-resolved density of state (DOS) of pyridine and pyridine–Ag<sub>2</sub>, where the OMOs and UMOs stand for occupied molecular orbitals and unoccupied molecular orbitals.

the pyridine–Ag<sub>2</sub> complex at the ground state, compared to those of pyridine (see data in Table 1). These changes in the electronic properties of the molecule will affect the nonresonance spectra. The calculated normal Raman spectrum of pyridine is shown in Fig. 3. Here, five important vibrational modes of pyridine and the pyridine–Ag complex (Fig. 4) are studied in the normal and the resonance case, respectively. Comparing directly the normal Raman spectrum of pyridine–Ag<sub>2</sub> with the normal Raman spectrum of pyridine, five enhanced same vibrational normal modes, 1010, 1049, 1249, 1504, and 1630 cm<sup>-1</sup> for pyridine–Ag<sub>2</sub> compared with those of pyridine were studied (Figs 3 and 4).

The enhancement in the normal Raman scattering factor ( $S_p$  in Eqn (2)) of pyridine–Ag<sub>2</sub> relative to that for pyridine in the absence of the cluster provides a direct measure of the static chemical (SC) enhancement. The rates of SC enhancement for these five vibrational modes are listed in Table 2. One can see that the SC enhancement rates of these five modes are different and all of them are less than 4 times. In the case of the same vibrational mode, the Raman wavenumbers of the pyridine–Ag<sub>2</sub> complex are also different from those of pyridine, which are blue shifted by about 50 cm<sup>-1</sup>. By analyzing these enhanced vibrational modes (Fig. 4), one important conclusion can be drawn: all the enhanced vibrational modes are the symmetric vibrational modes, and their orientation is consistent with the orientation of the permanent dipole moment and permanent polarizability at the ground states (along the molecule axis), i.e. consistent with the orientation of charge redistribution between pyridine and the metal.

**Table 1.** The calculated static dipole moments and static polarizabilities of the ground states with DFT/B3LYP/6-31G(D) for pyridine and DFT/B3LYP/LANL2DZ for pyridine–Ag. Their Cartesian coordinates are shown in Fig. 1

	Dipole moment ( <i>D</i> )			Polarizability (au)		
	<i>x</i>	<i>y</i>	<i>z</i>	<i>xx</i>	<i>yy</i>	<i>zz</i>
Pyridine	2.1063	-1.3167	0.0000	63.305	66.190	18.751
Pyridine–Ag	-7.7503	0.0005	0.4703	240.076	134.641	97.433

**Table 2.** The enhanced rates of intensities of Raman spectra by static chemical ( $G_{SC}$ ), CT ( $G_{CT}$ ), and intracluster excitation ( $G_{IE}$ ) enhancements. The vibrational modes a–e can be seen from Fig. 4

Vibrational modes	$G_{SC}$	$G_{CT}$				$G_{IE}$	
		785 nm	630 nm	514 nm	295 nm	370 nm	325 nm
a	3.05	3.43	$3.4 \times 10^2$	3.00	$3.3 \times 10^3$	$1.4 \times 10^4$	$3.7 \times 10^3$
b	1.20	1.78	3.70	4.41	$1.9 \times 10^2$	$1.7 \times 10^3$	$6.0 \times 10^3$
c	0.72	0.95	$7.5 \times 10^2$	1.57	$1.5 \times 10^4$	$1.1 \times 10^2$	$3.4 \times 10^3$
d	1.56	1.81	$1.5 \times 10^2$	1.34	$3.7 \times 10^3$	$1.7 \times 10^4$	$6.3 \times 10^4$
e	3.33	4.63	$1.7 \times 10^3$	8.71	$6.8 \times 10^3$	$1.3 \times 10^2$	$1.6 \times 10^3$

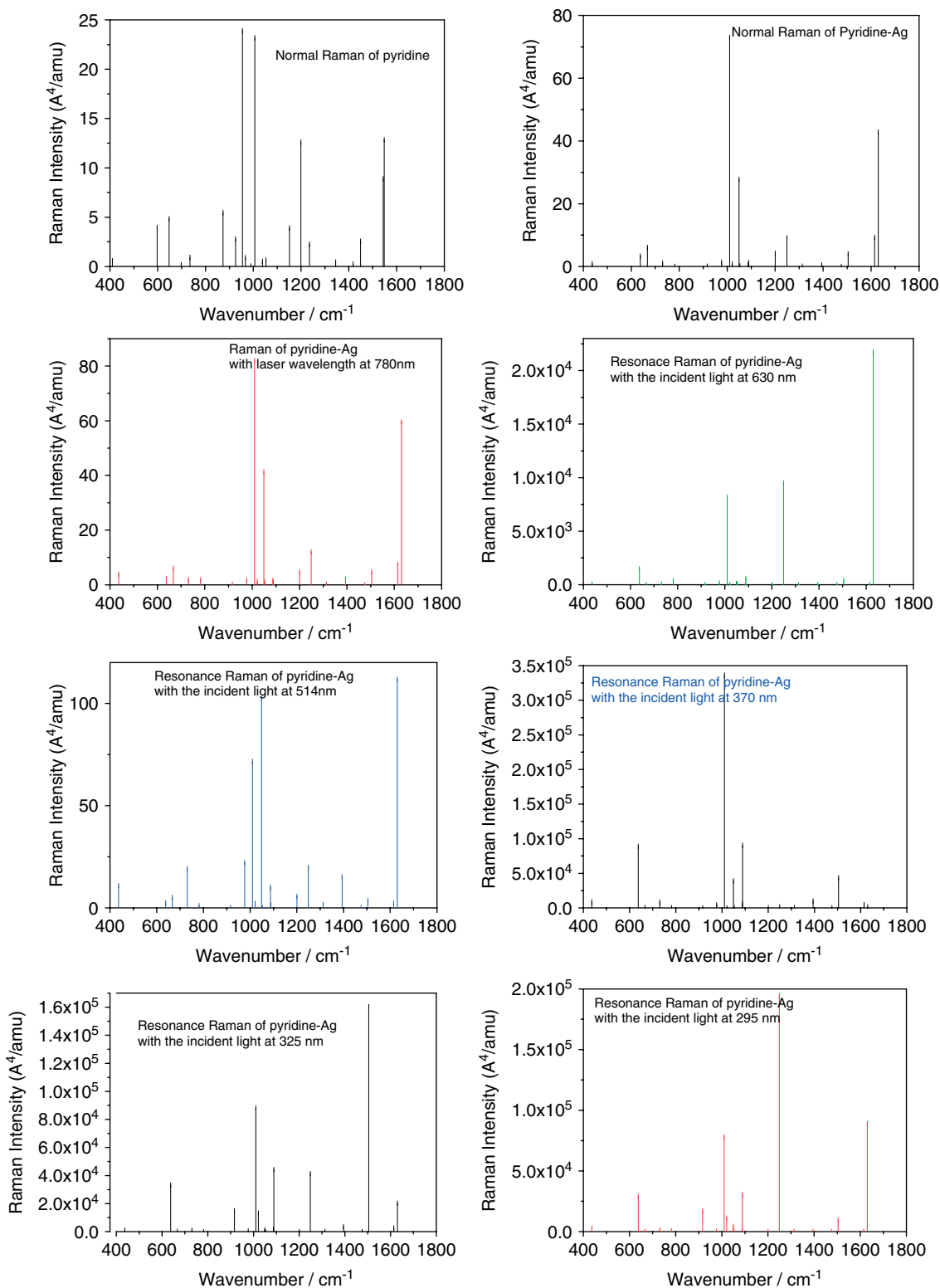
In the Raman scattering measurement, when the incident light is close to an electronic excitation of the molecule (which is adsorbed on the metal cluster), the intensity of the signal can be enhanced by a factor of up to  $10^4$ – $10^6$ .<sup>16,17</sup> This process is referred to as SERRS, and the enhancement is proportional to the oscillator strength of the transition.

Depending on the nature of the interaction between pyridine and the metal, the new metal–pyridine CT excited states could occur. Transition energies and oscillator strengths of pyridine and pyridine–Ag<sub>2</sub> for the lowest six singlet excited states are listed in Table 3. It should be noted that the absorption properties of the pyridine–metal cluster depend strongly on the cluster size.<sup>18</sup>

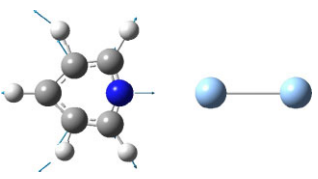
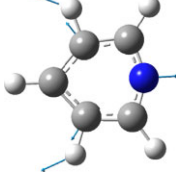
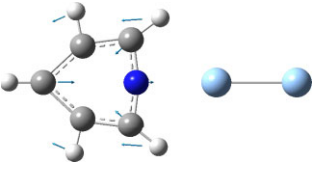
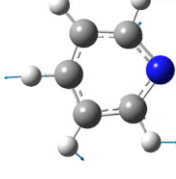
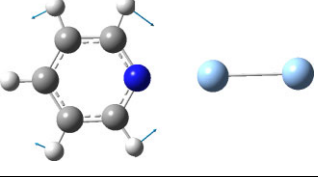
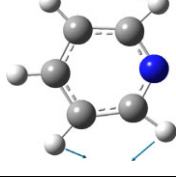
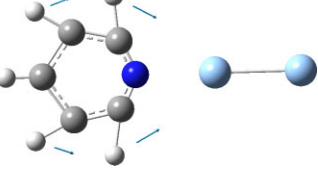
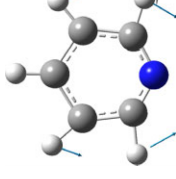
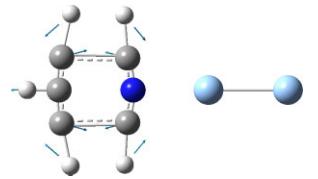
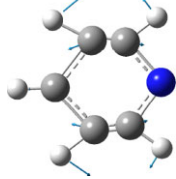
The  $S_1$  of pyridine–Ag<sub>2</sub> is much lower than the intrinsic intramolecular excitations (265.5 nm) because of the decrease of the band gap of the pyridine–Ag<sub>2</sub> complex (compared to that of pyridine), since  $S_1$  is contributed from the orbital transition HOMO → LUMO. The band gap in Fig. 2(b) is larger than the excitation energy of  $S_1$  in Table 3 for pyridine–Ag<sub>2</sub>, which can be interpreted with theories of CT exciton and the exciting binding energy.<sup>35,36</sup> The excited state properties of pyridine–Ag<sub>2</sub> are investigated with the charge difference density. From the charge difference densities of pyridine–Ag<sub>2</sub> (listed in Fig. 5),  $S_1$ ,  $S_2$ ,  $S_5$ , and  $S_6$  are the CT-excited states in absorption (electrons transfer from Ag<sub>2</sub> to pyridine) since as a result of CT, the holes and electrons are localized on Ag and pyridine, respectively. The transferred

**Table 3.** The calculated transition energies (TE) and oscillator strengths (*f*) of pyridine and pyridine–Ag<sub>2</sub> with TD-DFT/B3LYP/6-31G(D)//DFT/B3LYP/6-31G(D) and TD-DFT/B3LYP/LANL2DZ//DFT/B3LYP/LANL2DZ

	Pyridine		Pyridine–Ag <sub>2</sub>	
	TE (nm)	<i>f</i>	TE (nm)	<i>f</i>
$S_1$	265.51	0.0062	638.99	0.0003
$S_2$	252.42	0.0000	505.82	0.0000
$S_3$	218.56	0.0211	378.29	0.5784
$S_4$	187.44	0.0114	316.55	0.2651
$S_5$	163.32	0.4493	307.79	0.1719
$S_6$	161.96	0.4575	302.27	0.1537



**Figure 3.** The normal Raman spectra of pyridine and pyridine–Ag<sub>2</sub> and the resonance Raman spectra of pyridine–Ag with different incident light wavelengths. This figure is available in colour online at [www.interscience.wiley.com/journal/jrs](http://www.interscience.wiley.com/journal/jrs).

	cm <sup>-1</sup>	Vibrational modes	cm <sup>-1</sup>	Vibrational modes
a	1010		954.75	
b	1049		1006.29	
c	1249		1198.85	
d	1504		1449	
e	1630		1548.05	

**Figure 4.** The enhanced vibrational modes of pyridine and pyridine–Ag<sub>2</sub> for normal Raman scattering. This figure is available in colour online at [www.interscience.wiley.com/journal/jrs](http://www.interscience.wiley.com/journal/jrs).

electron resides for some femtoseconds in pyridine and after that returns to the metal cluster.

For the pyridine–Ag<sub>2</sub> complex, the resonance Raman spectra and the electronic polarizabilities were calculated with the laser wavelength 780, 630 and 514, 370, 325, and 295 nm, respectively. The energy of the incident light of 780 nm is lower than the S<sub>1</sub> electronic transition energy of pyridine–Ag<sub>2</sub> (638.99 nm), so the calculated result with 785 nm laser excitation is the normal Raman spectrum, and the experimental spectra should be from normal Raman scattering, and the large enhancement in the experiment should mostly result from EM enhancement since the calculated relative intensities of the Raman spectrum of pyridine–Ag<sub>2</sub> with the incident light at 780 nm are almost the same as those of pyridine–Ag without the incident light (normal Raman of pyridine–Ag<sub>2</sub>).

When the incident light is at 630 nm, it is almost resonant with the transition energies at the first excited state, which is the CT-excited state. The calculated intensities of the resonance Raman spectrum of pyridine–Ag<sub>2</sub> is much larger than that of the normal Raman spectrum of pyridine. It can be seen that the CT enhancement can reach the order of 10<sup>3</sup>, and the ring stretch mode at 1630 cm<sup>-1</sup> shows the largest enhancement, which is larger than that of the two ring breathing modes around 1000 cm<sup>-1</sup>, which is consistent with the order calculated by Zhao *et al.*<sup>17</sup> Arenas *et al.*<sup>14</sup> also analyzed the results theoretically by considering the displacements between the ground state of pyridine and its anion. Our calculations are in good agreement with their findings, particularly the very strong enhancement of the mode at 1573 cm<sup>-1</sup>. When the laser wavelength is 514 nm, though this laser energy almost resonates with the

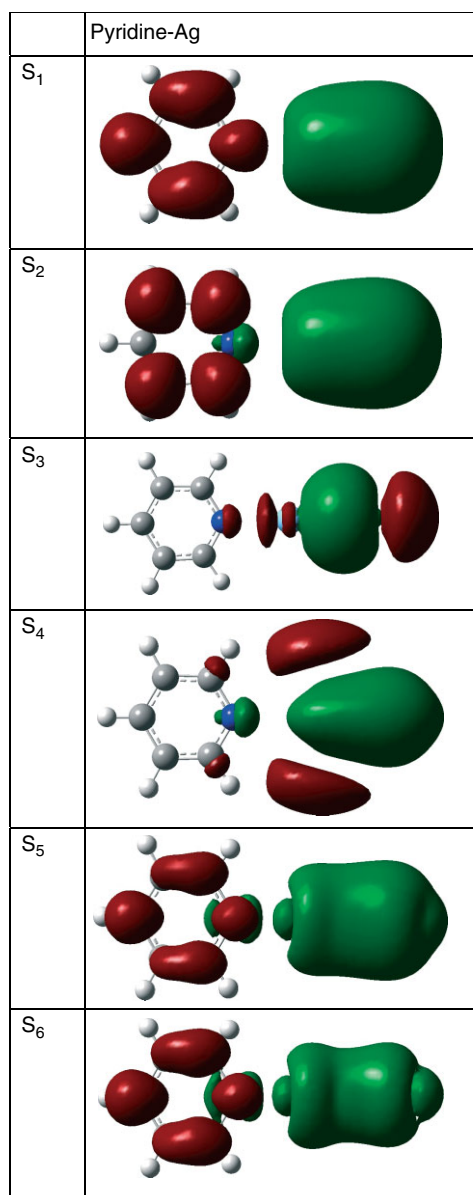


**Figure 5.** The charge density differences of pyridine–Ag<sub>2</sub> for the first six singlet excited states, where the green and red stand for the hole and the electron, respectively.

transition energy of  $S_2$ , the intensity of resonance Raman bands is not enhanced strongly (less than 10 times compared to the intensity of the normal Raman of pyridine (see data in Table 2)). The reason is that the oscillator strength  $f = 0.0000$  for this excited state. The calculated resonance Raman spectrum with the incident light of 295 nm can be seen in Fig. 3, and the enhanced rates are listed in Table 3. It can be seen that the largest enhancement is of the order of  $10^4$ . Note that the incident light at 295 nm is near-resonant with the  $S_6$  excited state (302 nm). If the incident light is in exact resonance with 302 nm, the enhancement will be larger than the calculated result with the incident light at 295 nm.

**Table 4.** The wavenumber-dependent polarizabilities of pyridine–Ag<sub>2</sub> in atomic units (a.u.). Their Cartesian coordinates are listed in Fig. 1

Wavelengths of laser (nm)	$xx$	$yy$	$zz$
780	246	107	181
630	273	107	195
514	335	125	225
370	–1800	200	–460
325	86	439	574
295	–24.5	–589	81

From Fig. 4, when the excitation wavelength is resonant with the strong electronic intracluster excitations ( $S_3$  and  $S_4$ ), they are the localized excited states (all the electrons and hole are localized on the metal cluster, and there is CT within the metal cluster); there is no CT between Ag<sub>2</sub> and pyridine.  $S_3$  is a 5s bonding to 5s antibonding transition in Ag<sub>2</sub>.  $S_4$  is a 5s to 5p atomic transition within the first Ag atom bonded to pyridine. The excited metal cluster shows a larger transition dipole moment and wavenumber-dependent polarizability (Table 4), but with different orientations. The large transition dipole moment and wavenumber-dependent polarizability on the metal cluster can of course strongly enhance the intensity of SERRS. This type of contribution from the resonant electronic intracluster excitations can be considered as the local field effect by collective plasmons. The difference is in the orientation of transition dipole and wavenumber-dependent polarizability. For  $S_3$  the orientation is along the molecular axis (perpendicular the metal surface), so the largest enhancement of SERRS is  $10^4$  times by collective plasmons. There is an angle between the metal surface and the orientation of the transition dipole for  $S_4$ , so the enhancement of SERRS along the molecular axis by collective plasmons is less, and the order of the largest enhancement is  $10^3$  times for the considered five important modes (Table 2). It should be noted that the vibrational mode at  $1504\text{ cm}^{-1}$  is significantly enhanced, and the enhanced factor is  $2.5 \times 10^4$ ; the reason is that the orientation of the vibrational mode is along the orientation of the transition dipole moment (or polarizability) (Figs 4 and 5). The selection rule of SERRS for this type of enhanced mechanism is  $I \propto I_{\text{max}} \cos^2(\theta)$ , where  $\theta$  is the angle between the orientation of molecular vibration and the orientation of the polarizability within cluster, and  $I_{\text{max}}$  is the intensity at  $\theta = 0^\circ$ . So, the enhancement of SERRS by collective plasmons depends on the orientation of the transition dipole and frequency-dependent polarizability in clusters. It should be noted that strong intracluster excitations ( $S_3$  and  $S_4$ ) yield high Raman scattering from pyridine via a type of Förster excitation transfer.

## CONCLUSIONS

Depending on the nature of the interaction between pyridine and metal, the new metal–pyridine CT excited states have been visualized directly by charge difference density. The order of the CT enhancement can be up to the order of  $10^4$  for the pyridine–Ag<sub>2</sub> complex. The strong intracuster resonance excitations were also shown with charge difference density. These strong intracuster resonance excitations yield high Raman scattering from pyridine via a type of Förster excitation transfer. The enhancement of SERRS by local field effects of collective plasmons depends on the orientation of transition dipole and wavenumber-dependent polarizability in the metal cluster, and the enhancement can be up to the order of  $10^4$  for the pyridine–Ag<sub>2</sub> complex. The selection rules for the SERRS have been obtained for these two types of enhancement mechanisms.

## Acknowledgements

This work was supported by the National Natural Science Foundation of China (Grant Nos: 10625418, 20673012 and 20703064), the National Basic Research Program of China (Grant Nos: 2007CB936801 and 2007CB936804), the Sino-Swedish collaborations about nanophotonics and nanoelectronics (2006DFB02020), and the 'Bairen' projects of CAS.

## REFERENCES

- Jeanmaire DL, Van Duyne RP. *J. Electroanal. Chem.* 1977; **84**: 1.
- Albrecht MG, Creighton JA. *J. Am. Chem. Soc.* 1977; **99**: 5215.
- Moskovits M. *Rev. Mod. Phys.* 1985; **57**: 783.
- Kneipp K, Kneipp H, Itzkan I, Dasari RR, Feld MS. *Chem. Rev.* 1999; **99**: 2957.
- Kneipp K, Kneipp H, Moskovits M. *Surface-enhanced Raman Scattering, Physics and Applications*. Springer: Heidelberg, 2006.
- Persson BNJ. *Chem. Phys. Lett.* 1981; **82**: 561.
- Adrian FJ. *J. Chem. Phys.* 1982; **77**: 5302.
- Kambhampati P, Child CM, Foster MC, Campion A. *J. Chem. Phys.* 1998; **108**: 5013.
- Persson BNJ, Zhao K, Zhang ZY. *Phys. Rev. Lett.* 2006; **96**: 207401.
- Bjernelid EJ, Svedberg F, Johansson P, Kall M. *J. Phys. Chem. A* 2004; **108**: 4187.
- Otto A, Mrozek I, Grabhorn H, Akemann W. *J. Phys. Condens. Matter* 1992; **4**: 1143.
- Campion A, Ivaneky JE, Child CM, Foster M. *J. Am. Chem. Soc.* 1995; **117**: 11807.
- Arenas JF, Woolley MS, Otero JC, Marcos JI. *J. Phys. Chem.* 1996; **100**: 3199.
- Arenas JF, Tocón IL, Otero JC, Marcos JI. *J. Phys. Chem.* 1996; **100**: 9254.
- Lombardi JR, Birke RL, Lu T, Xu J. *J. Chem. Phys.* 1986; **84**: 4174.
- Zhao LL, Jensen L, Schatz GC. *Nano Lett.* 2006; **6**: 1229.
- Zhao LL, Jensen L, Schatz GC. *J. Am. Chem. Soc.* 2006; **128**: 2911.
- Jensen L, Zhao LL, Schatz GC. *J. Phys. Chem. C* 2007; **111**: 4756.
- Vivoni A, Birke RL, Foucault R, Lombardi JR. *J. Phys. Chem. B.* 2003; **107**: 5547.
- Aikens CM, Schatz GC. *J. Phys. Chem. A* 2006; **110**: 13317.
- Campion A, Mullins DR. *Chem. Phys. Lett.* 1983; **94**: 576.
- Weaver MJ, Farquharson S, Tadayyon MA. *J. Chem. Phys.* 1985; **82**: 4867.
- Zuo C, Jagodzinski PW. *J. Phys. Chem. B* 2005; **109**: 1788.
- Centeno SP, López-Tocón I, Arenas JF, Soto J, Otero JC. *J. Phys. Chem. B* 2006; **110**: 14916.
- Thomas S, Biswas N, Venkateswaran S, Kapoor S, Naumov S, Mukherjee T. *J. Phys. Chem. A* 2005; **109**: 9928.
- Arenas JF, López-Tocón I, Castro JL, Centeno SP, López-Ramírez MR, Otero JC. *J. Raman Spectrosc.* 2005; **36**: 515.
- Li XY, Huang QJ, Petrov VI, Xie YT, Luo Q, Yu XG, Yan YJ. *J. Raman Spectrosc.* 2005; **36**: 555.
- Sun MT. *J. Chem. Phys.* 2006; **124**: 054903.
- Sun MT, Kjellberg P, Beenken WJD, Pullerits T. *Chem. Phys.* 2006; **327**: 474.
- Sun MT, Liu LW, Ding Y, Xu HX. *J. Chem. Phys.* 2007; **127**: 084706.
- Frisch MJ, Trucks GW, Schlegel HB, Scuseria GE, Robb MA, Cheeseman JR, Montgomery JA, Vreven T Jr, Kudin KN, Burant JC, Millam JM, Iyengar SS, Tomasi J, Barone V, Mennucci B, Cossi M, Scalmani G, Rega N, Petersson GA, Nakatsuji H, Hada M, Ehara M, Toyota K, Fukuda R, Hasegawa J, Ishida M, Nakajima T, Honda Y, Kitao O, Nakai H, Klene M, Li X, Knox JE, Hratchian HP, Cross JB, Adamo C, Jaramillo J, Gomperts R, Stratmann RE, Yazyev O, Austin AJ, Cammi R, Pomelli C, Ochterski JW, Ayala PY, Morokuma K, Voth GA, Salvador P, Dannenberg JJ, Zakrzewski VG, Dapprich S, Daniels AD, Strain MC, Farkas O, Malick DK, Rabuck AD, Raghavachari K, Foresman JB, Ortiz JV, Cui Q, Baboul AG, Clifford S, Cioslowski J, Stefanov BB, Liu G, Liashenko A, Piskorz P, Komaromi I, Martin RL, Fox DJ, Keith T, Al-Laham MA, Peng CY, Nanayakkara A, Challacombe M, Gill PMW, Johnson B, Chen W, Wong MW, Gonzalez C, Pople JA. *GAUSSIAN 03*, revision B. 05. Gaussian Inc.: Wallingford, 2004.
- Wu DY, Hayashi M, Lin SH, Tian ZQ. *Spectrochim. Acta. A* 2004; **60**: 137.
- Neugebauer J, Reiher M, Kind C, Hess BA. *J. Comput. Chem.* 2002; **23**: 895.
- Neaton JB, Hybertsen MS, Louie SG. *Phys. Rev. Lett.* 2006; **97**: 216405.
- Hill IG, Kahn A, Soos ZG, Pascal RA Jr. *Chem. Phys. Lett.* 2000; **327**: 181.
- Alvarado SF, Seidler PF, Lidzey DG, Bradley DDC. *Phys. Rev. Lett.* 1998; **81**: 1082.